



Bulletin of the Mineral Research and Exploration

<http://bulletin.mta.gov.tr>



GIS-based analytical hierarchy process, weight of evidence and logistic regression models for the landslide susceptibility predicting in Echorfa Region (northwestern of Algeria)

Zine El Abidine ROUKH^{a*} and Abdelmansour NADJI^a

^aOran 2 Mohamed Ben Ahmed University, Faculty of Earth Science and the Universe, Laboratory of Georesources, Environments and Natural Risks, El-M'Naouar, Oran, 31000, Algeria

Research Article

Keywords:

Analytical Hierarchy Process, Landslide, Logistic Regression, Susceptibility Mapping, Weight of Evidence.

ABSTRACT

The main objective of this study is destined to combine the Analytical Hierarchy Process (AHP), Weight of Evidence (WOE), Logistic Regression (LR) methods and geographic information system (GIS) to predict landslide susceptibility of the Echorfa region (northwestern of Algeria). Nine factors such as slope, aspect, lithology, distance to faults, lineaments density, distance to the streams, precipitations, land use and altitude are included in landslide susceptibility evaluation process. A detailed landslide inventory map was established by satellite images and filed surveys. Three landslide susceptibility maps are established using the different statistical models. Five landslide susceptibility categories are generated by the GSI classification nil, low, moderate, high and very high susceptibility. The performance of the different models in landslide susceptibility is calculated based in the area under curve of the Receiver Operating Characteristic (ROC) which give a satisfactory result. The results showed that the WOE is more performance than the two other techniques. The produced landslide susceptibility maps provide important spatial information about landslide prone area, where the constructed map's content will help the decision makers in land use planning.

Received Date: 15.08.2021

Accepted Date: 10.12.2021

1. Introduction

Landslides are geodynamic phenomena that occur in many part of the world and often the most severe on the earth surface. They cause changes to the landscape and can destroy building, structures and sometimes it reaches catastrophic levels and cause a death. These slope movements occur during earthquake, and /or during intense rainy periods with prolonged precipitation and the combined action of various geomorphological factors (Roukh, 2020).

This problem is currently one of the major concerns of the scientists responsible for the geological risks management. Nowadays, landslide

susceptibility mapping become a consistent method used in landslide prone area zoning. This technique is based in the application of quantitative, semi quantitative and qualitative models to calculate spatial distribution of the landslide susceptibility index (LSI). Several guidelines are developed in the term of landslide susceptibility, hazard and risk zoning for land use planning destined to local, state and national government officials, land use planners, geotechnical professionals and project managers (Flentje et al., 2007; Fell et al., 2008)

In the practice, several models based on geographic information system are used in the

Citation Info: Abidine Roukh, Z. E., Nadji, A. 2023. GIS-based analytical hierarchy process, weight of evidence and logistic regression models for the landslide susceptibility predicting in Echorfa Region (northwestern of Algeria). Bulletin of the Mineral Research and Exploration 170, 31-55. <https://doi.org/10.19111/bulletinofmr.1035480>

*Corresponding author: Zine El Abidine ROUKH, zinougeorisque@gmail.com

landslide susceptibility mapping. The bivariate statistical methods is largely used for evaluate landslide susceptibility versus authors (Süzen and Doyuran, 2004; Mohammady et al., 2012; Zine El Abidine and Abdelmansour, 2019). The multivariate statistical models are also integrated in several works related to landslide susceptibility zoning, (Baeza and Corominas, 2001; Santacana et al., 2003; Ercanoğlu et al., 2004), machine learning ensemble (Micheletti et al., 2014; Pham et al., 2017; Chen et al., 2018). Artificial neural network (ANN) models are applied in calculation weights for landslide susceptibility (Lee et al., 2004; Yilmaz, 2009; Zare et al., 2013). Others researches are compared several models to selected the adopted landslide susceptibility model (Xu et al., 2012; Bourenane et al., 2016; Chen et al., 2017; Merghadi et al., 2018; Mahdadi et al., 2018; Karim et al., 2019).

The favorable geological, geomorphological and climatic conditions make certain regions located in northern part of Algeria prone to landslides phenomena; these phenomena cause annual few human losses and considerable damage in term of basic infrastructure such as highways, private and state property (Guemache et al., 2011; Djerbal et al., 2017; Achour et al., 2017; Hallal et al., 2019). Attempts have been made to the landslide susceptibility mapping (Bourenane et al., 2015; Hadji et al., 2017; Dahoua et al., 2017; El Mekki et al., 2017; Mahdadi et al., 2018; Zine El Abidine and Abdelmansour, 2019; Karim et al., 2019; Roukh, 2020). However, these studies are insufficient in relation to the large area of this part of the country.

The objective of this study is to establish a comprehensive methodology based on the exploitation of multi - source data in order to the landslide susceptibility mapping of the Echorfa sector sited in Oran region (north western of Algeria). Therefore, an integrated analytical approach consists of: i) the establishment of database contains the landslide causative factors and landslide inventory, ii) the estimation of the weighting of each parameter by integration of the AHP, WOE and LR methods coupled with GIS functionalities, iii) the evaluation and the mapping of the landslide susceptibility and iv) validation and interpretation of the obtained results.

2. General Characteristic of the Study Area

The study area is part of the Beni Chougrane Mountains sited in northwestern of Algeria (Figure 1a). It's located at the intersection of eight municipalities: Sig, Zahana, Echorfa, El Gaada, Ogaz (Wilaya of Mascara), Makedra (W. Sidi Bel Abbes) and Oued Tlelat and Tafraoui municipality (W. Oran) (Figure 1b). This zone covers an area of 408 km² and a total perimeter of 89.761 km². It is located exactly between the longitude (727595.762, 760285.913) and latitude (3923356.604, 3937796.033 according to (WGS_1984_UTM_Zone 30N) coordinate projection system.

The Bas Chelif basin is part of the western Algerian sublittoral Neogene basins. The significant Neogene sedimentation covers the western part of this intra-mountainous basin, of which the Miocene covers the vast majority of the deposits. It is surrounded by the northern foothills of the Dahra and the Arzew mountains, and by the mountains of Tessala and Beni Chougrane and the secondary-age Ouarsenis massif to the south, which provides it with material through erosion. The study area is part of the Lower Chelif Cenozoic sedimentary complex. According to the geological map (Figure 2), three regions are distinct: i) a mountainous area corresponds to an antero-genic period occupying the southwestern half of the map, ii) a plateau area visible on the northwestern part of the map occupied by the plain of M'Léta. From the litho - stratigraphic point of view: i) The secondary represented by shales and marl of Cretaceous age constitutes the substratum of a Cenozoic cover. This substratum is visible in the valley of Oued Makedra and in the depression west of the lauriers roses, these are black - grey marly limestones intercalated with hard fine - paste limestone banks, ii) the Cenozoic is mainly located in the southern part of the map, and it is represented by the Neogene formations. The Miocene: it is typically transgressive deposits on secondary terrain such as the following formations; Middle Miocene: a sequence of detritus, siltstones, sandstones and gray argillite conglomerates (200 m thick). The Upper Miocene: the base levels of the Miocene series are generally detrital and represented by silts and red conglomerates resting on a thin lithological formation of cinerite, these formations are particularly well developed in Djebel Touakes,

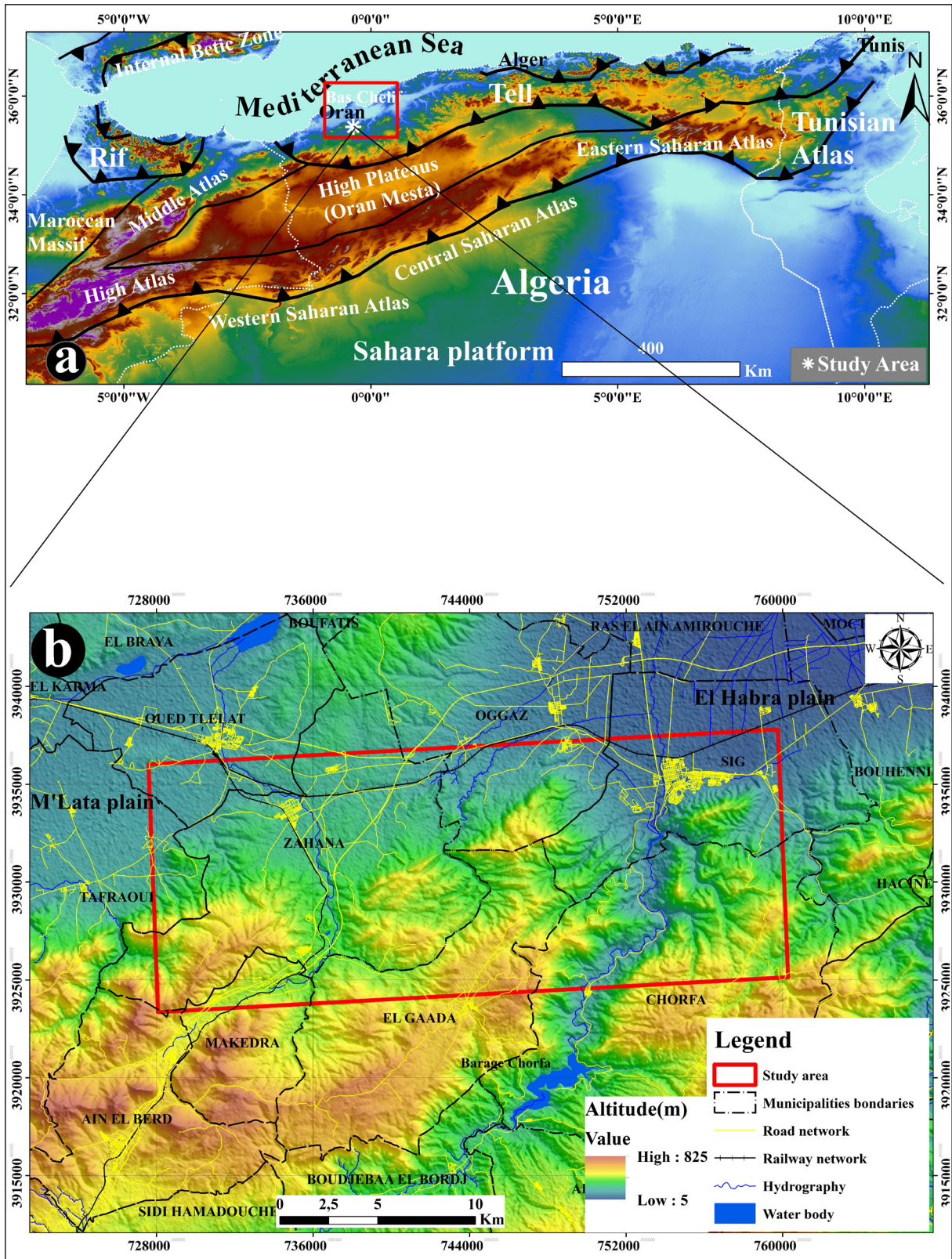


Figure 1- a) Geographic position of the study area versus the Chelif basin northwestern of Algeria, b) geographic location versus municipalities division of the NW of Algeria.

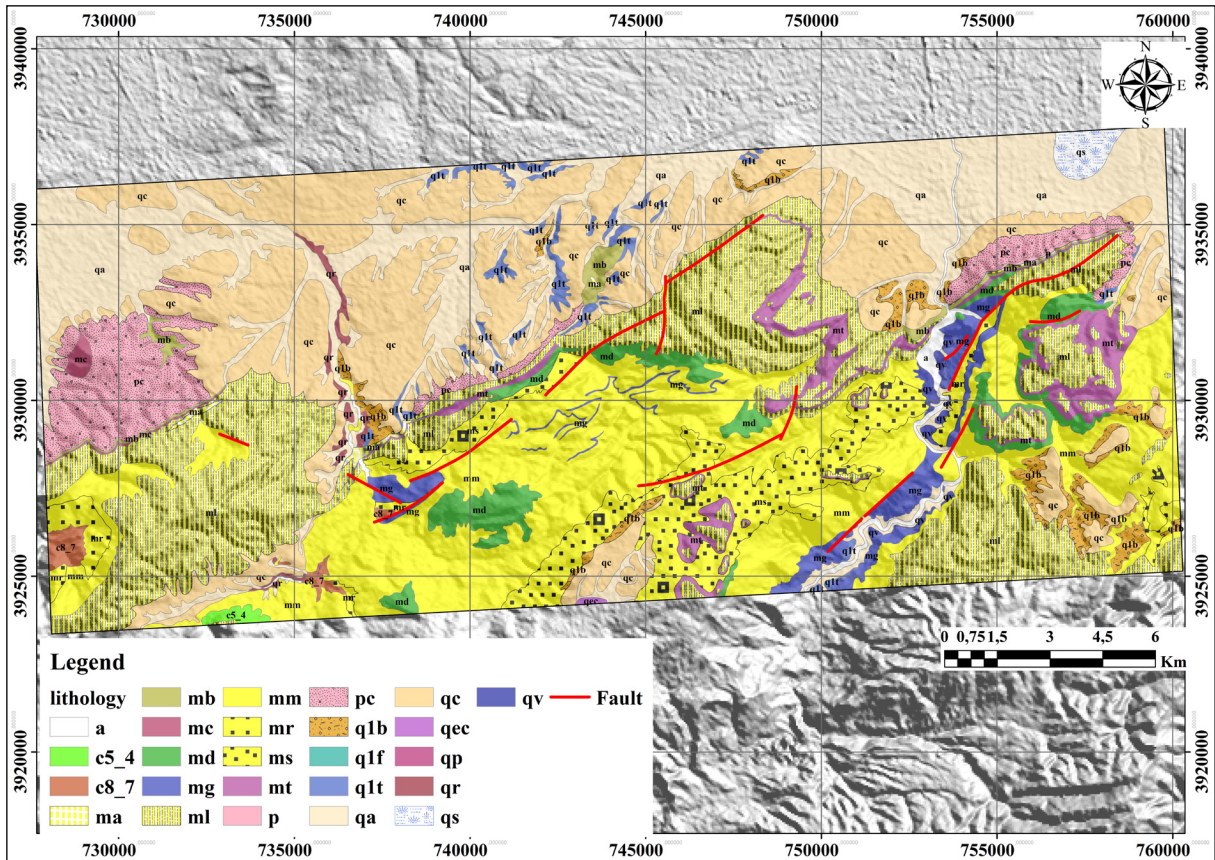


Figure 2- Geological map of the study area (digitized by 1/50000 scale geological map of the St Denis-Du- Sig, Sheet N°182, B10 C7).

above which plastic blue marls have been found containing a microfauna characteristic of the upper Miocene and finally the series ends with gypsum and gypsum - marly, iii) The Pliocene: discordant with previous formations appears: Lower / Middle Pliocene (Calabrien): represented by reddish sandstones well cemented down to tender limestones and sandy marls of which the latter are part of marine formations. Upper Pliocene: it is a heterogeneous alternation of marl, sand silts and conglomerates (continental formations); iv) the Quaternary: the Quaternary formations occupies all northwest and northeast of the map, they are represented by: Early Quaternary corresponding to a calcareous carapace hiding the subjacent terrain. Recent Quaternary represented by non - rudoinous argilo - limoneous alluvial named recent alluvial. The current forms the major bed rivers.

The study area is defined by four morphological units: i) a mountainous area in the south of the plain represented by the Tessala Mountains and those of Beni Chougrane; ii) a depression zone in the

northwest represented by the M'Leta plain; iii) another depression zone located in the NE represented by the El Habra Plain, iv) an area of the plateaus located in the center represented by the Zahana and Sig plateaus.

The study area is located in the intersection of three sub-watersheds (Figure 3), the Sebkhia of Oran watershed code 04 - 04, El Habra watershed code 11 - 06 and the Echorfa watershed code 11 - 04. The hydrographic network characterized by a high density where the main rivers in this area that of Oued El Mebtouh which feeds the Mactaa swamps and the second river that of Oued Tlelat whose runoff reaches at Dayat Oum Ghezal.

The climate of the study area compared to the country's climate is characterized by a contrasting climate, a Mediterranean climate on the coast and desert climate in the south. The Mascara region is located in the Oran high plains; addressed as intermediate, hot and dry in summer, cold and rainy in winter. The average monthly precipitation during

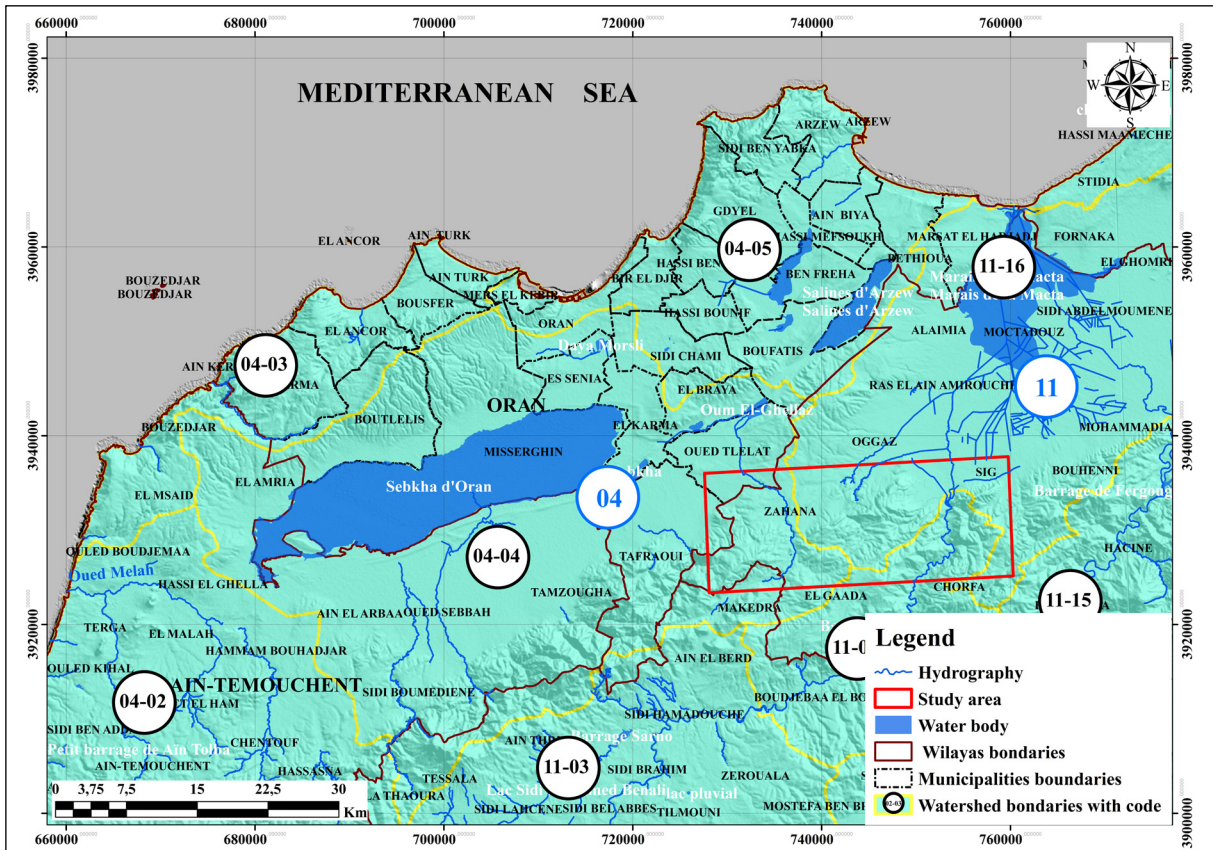


Figure 3- Hydrographic characteristics of the study area (watershed boundaries digitized by the 1/500.000 scale hydro - climatological network and water quality monitoring of the north Algerian).

the reference period (1982 - 2012) of the Echorfa Dam station (ANRH), was taken as reference. The average monthly precipitation study has shown that the rainy period begins in the October and split ends in April. During this period, it was noted maximum precipitation appears in November (56.0 mm) and for the minimum in July (1.4 mm). The average annual precipitation study allows us to note that: the rainiest year is recorded 514.9 mm; however, the driest year with a rainfall of 153.0 mm. The temperature together with precipitation is a major parameter that defines the climate of region; it is also one of the essential terms in the definition of the flow deficit. For our study area, the Mascara station is the only one where we were able to have a measurements series of this parameter during 2003 and 2012. Maximum temperatures in summer according to the exploitation of the ONM data, a maximum of 27.98 °C in July and the cold winter season with a minimum of 9.04 °C in January. The climatic regime of the study area is semi - arid.

The study area is part of the Algeria's Tellian Atlas belt belonging to the limit of the Africa - Eurasia tectonic plate which forms a deformed plug about 100 km wide. The North western of Algeria has an experienced several earthquakes and is among the 09/10/1790 Oran earthquake with an macro intensity of $I = X$ (Bouhadad and Laouami, 2002; Marinas and Salord, 1991). The 1819 Mascara events with an intensity of $I = X$ and that of 1851 with an macro intensity of $I = VIII$ (Guessoum et al., 2018). Recently, significant earthquakes are recorded at the Echorfa surroundings region, the Hassine (Mascara) earthquake of August 1994 with a magnitude of moment $M_w = 5.7$ (Benouar et al., 1994; Ayadi et al., 2002) and those of Ain Temouchent (December 1999, $M_w = 5.7$) and Oran (Juan 2008, $M_w = 5.5$) (Belayadi et al., 2017). According to Thomas (1985), the study area is located in the Beni Chougrane zone characterized by NE - SW reverse fault, where in the El Habra and M'Lata plains the direction of the reverse faults is NW - SE. Therefore, the study area characterized by significant

seismicity due to several active faults (Figure 4). The spatiotemporal distribution of these events plays a very important role in slope movements triggering or reactivating.

3. Landslide Susceptibility Mapping

In this work, an adopted methodology is established for the purpose of the landslide prone areas zoning. This approach consists firstly to establishing a set of thematic maps (data collection of the landslide causative factors and landslide inventory map). Secondly, an assessment of the landslide susceptibility index using AHP, WOE and LR models and GIS environment. Thirdly, mapping the LS by the classification of the GSI and validating of the obtained results. The following flowchart represents the methodology used in this work (Figure 5).

3.1. Landslide Inventory Mapping

Landslide inventory map present the essential parameter in the landslide susceptibility mapping (Fell et al., 2008; Corominas et al., 2014). In this study, an inventory map is established by the interpretation of the Google Earth satellite images as well as the field surveys and the positioning via Global Positioning System (GPS) area (Figure 6). It is mentioned that no landslide inventory maps are established in the study area. The objective of this inventory is to identify, localized and describe the main slope movements that occurred in the study area as well as to build and to calculate the performance of landslide susceptibility models.

3.1.1. Example of Some Remarkable Landslide

The expertise in - situ present a fundamental step in

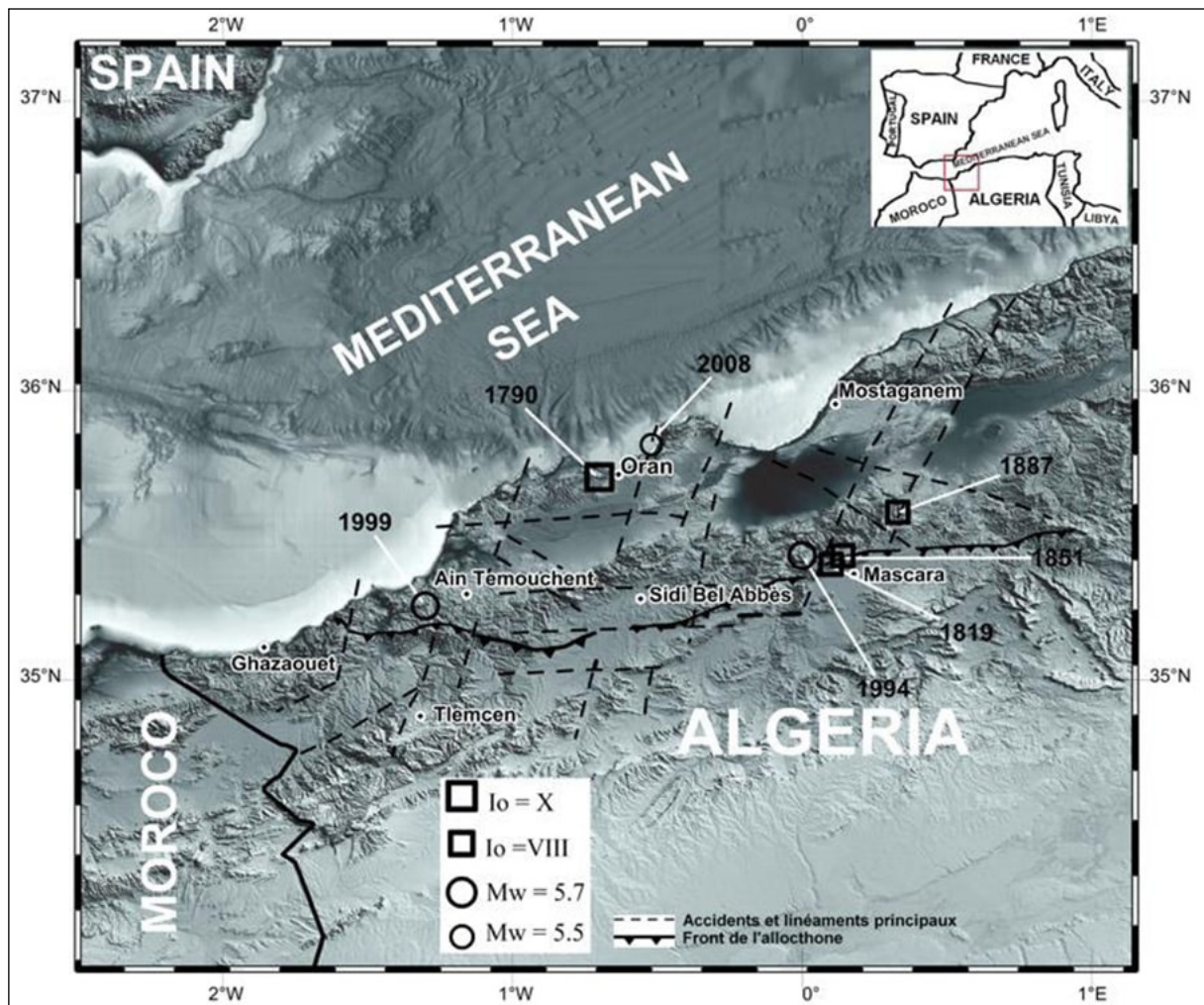


Figure 4- Main tectonic structure (Thomas, 1985) and relevant earthquakes that took place in Norwest Algeria (Belayadi et al., 2017).

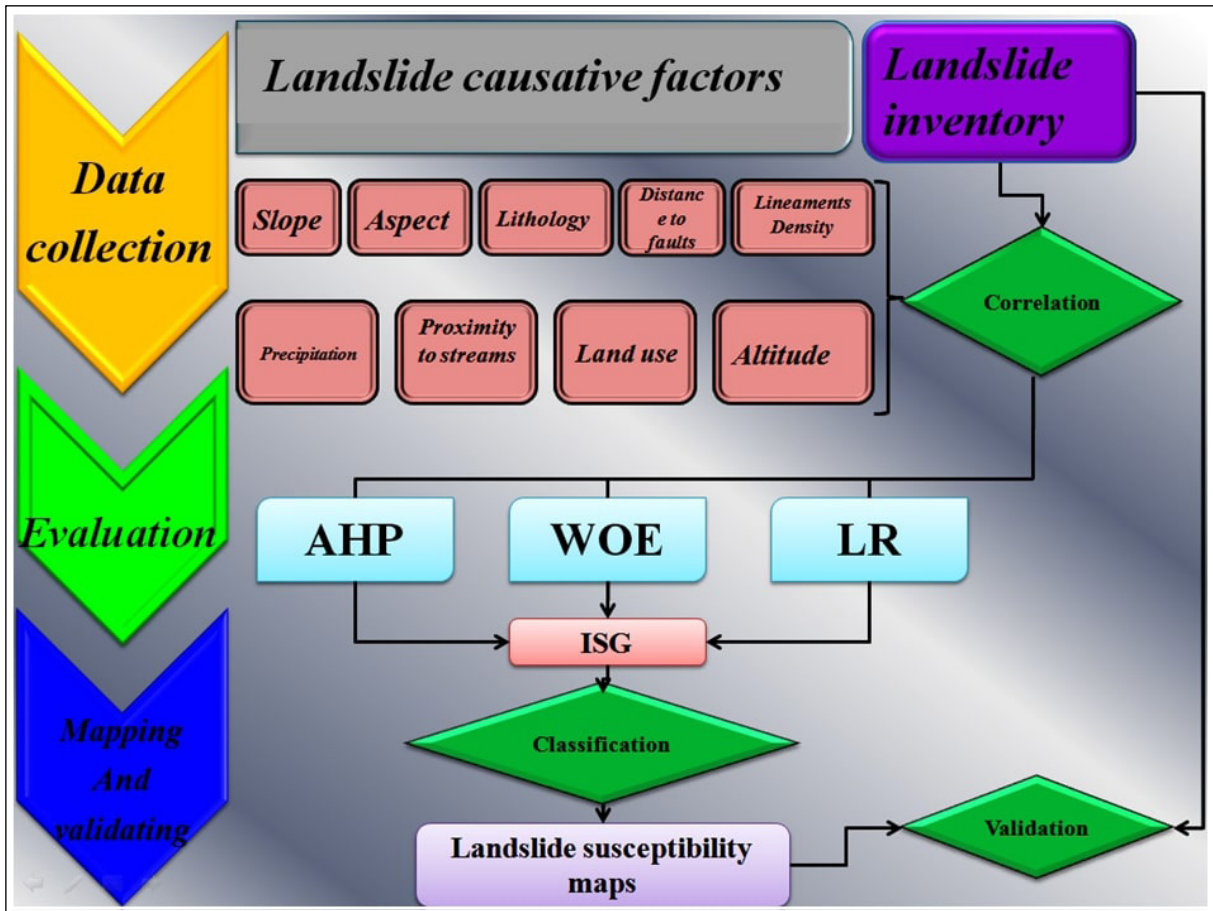


Figure 5- Methodology flowchart for the process work.

the landslide inventory, of which the geologist expert is able to identify, localized measure the affected site and to verify the landslides inventoried by the interpreting of the aerial photos, satellite images, archive, press or the previous documents. In this work, the extensive field surveys allowed us to identify several landslides (Figure 7).

Some examples are discussed in the following paragraph:

A rotational landslide is located using the Google Earth satellite images (Figure 7a) it occupies an area of 8.2 Ha. Among the instability index observed are those deviations of the river trajectory and remarkable degradation in the topography.

A second rotational landslide is identified from the Google Earth images (Figure 7b); it's characterized by main and minor scarp, a sliding surface and an ablation zone. The area of this landslide is approximately 9 Ha.

A third translational landslide type is identified via the GPS during the field surveys (Figure 7c).

A rotational landslide is identified near the road (towards the Echorfa town) whose the observed coordinates are (X_UTM = 752259.7, Y_UTM = 3931563.93) (Figure 7d).

A toppling affected the limestone formations are observed near El Gaada town. The coordinates of the site are (X_UTM = 751309.02, Y_UTM = 3930215.64) (Figure 7e).

An old complex landslide affected the marl-limestone formation is identified from the Google Earth images and verified on the field (Figure 7f). The area of the landslide is 6.4 Ha.

A rock fall of limestone formations are observed next to the road leading from Sig to Echorfa town (Figure 7g). The observe coordinats of the slope

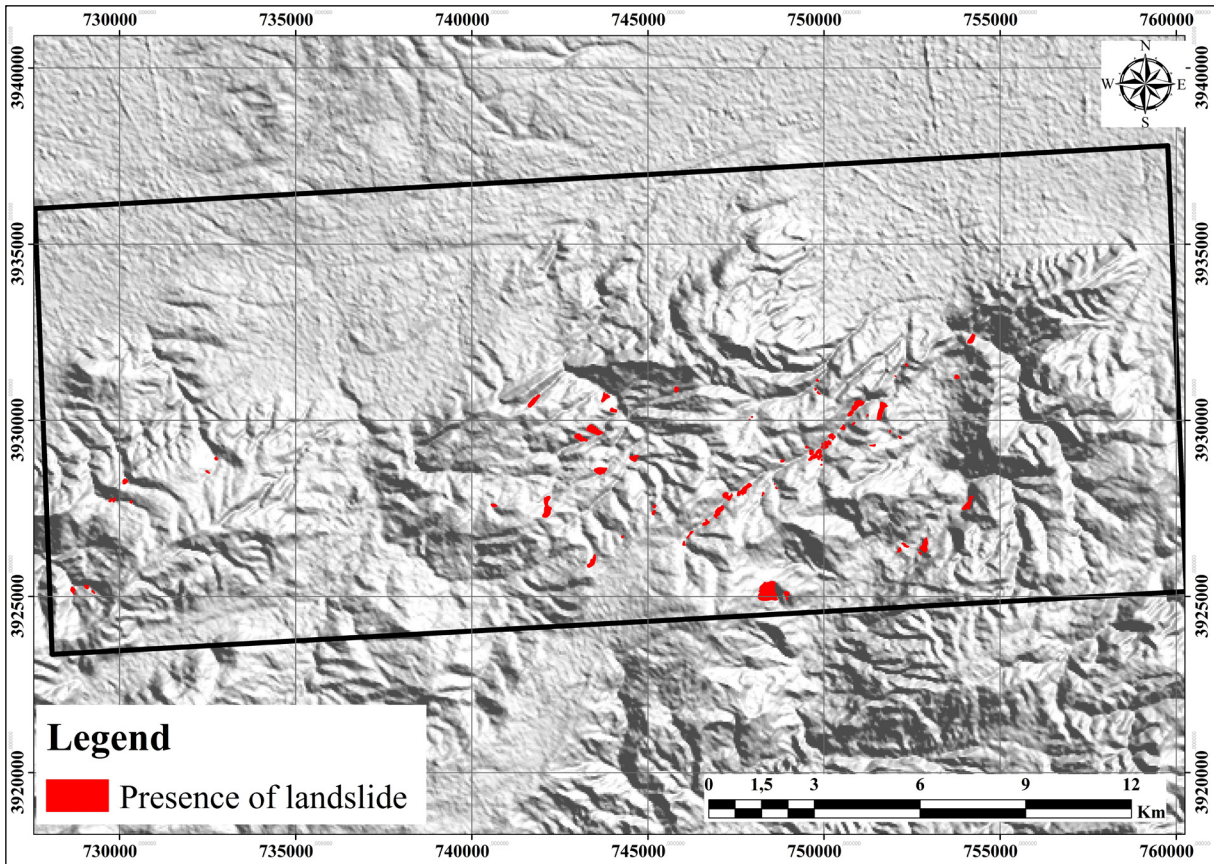


Figure 6- Landslide inventory map.

movement are ($X_{UTM} = 752312.21$, $Y_{UTM} = 3931540.77$).

According to Cruden and Varne (1996) classification, the slope movements concerned by this inventory are exclusively those which relate to the following phenomena: toppling, landslide (rotational translational and complex) and rock falls. In this research, landslides are used to construct landslide susceptibility maps which sampling in 70% of the total for models building and 30% for validation.

3.2. The Landslide Causative Factors

The processes behind landslides are very complex and diverse; geology, the relief and the slope exposure are more or less constant fundamental parameters over long period. Several factors can have a destabilizing influence on a slope such as slope, slope aspect, stratigraphy, distance to faults, the lineaments density, the altitude levels, and distance from the streams and other triggering factors related to the precipitation and

the groundwater circulation as well as earthquakes which trigger or reactivate ground movements.

In this study nine parameters are integrated into a GIS environment such as, slope, aspect, lithology, lineaments density, and distance to faults, precipitation and distance to the streams, land use and altitude in order to assess the landslide susceptibility index.

3.2.1. Slope Degree

Presents a fundamental parameter in the landslide susceptibility evaluation, the variation of the slope directly influence in the landslide process, in this context the slope map (Figure 5a) is derived from the digital elevation model (DEM) of the study area and it reclassified into five classes ($0 - 10^\circ$), ($10 - 20^\circ$), ($20 - 30^\circ$), ($30 - 40^\circ$) and $> 40^\circ$ using the ArcGIS software modules (Figure 8a).

3.2.2. Slope Aspect

This factors influences in the slope instability by the soil concentration moisture changes according to

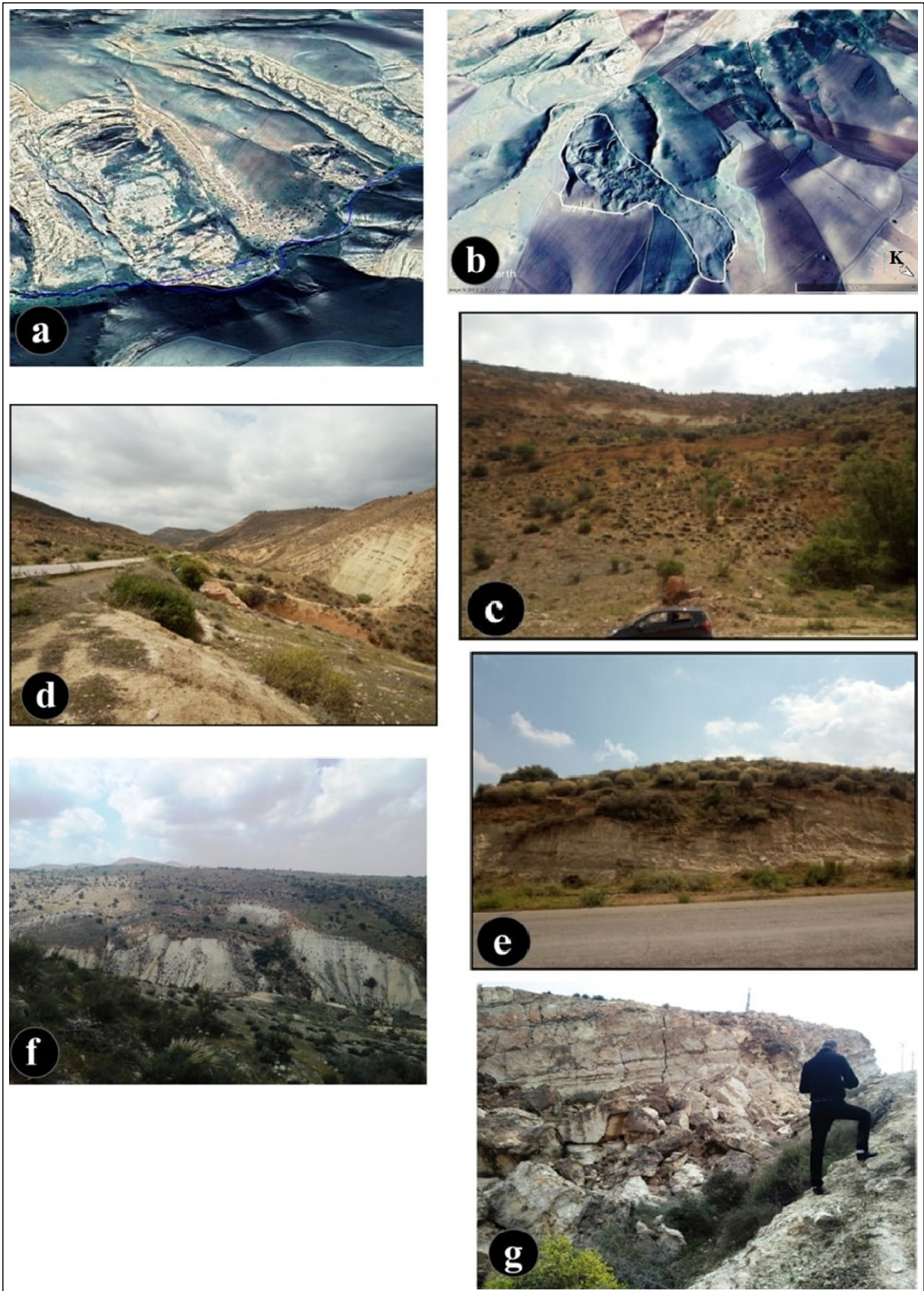


Figure 7- Example of some remarkable landslide inventoried in the study area; a) Active rotational landslide, b) rotational landslide identified by Google Earth, c) translational landslide, d) rotational landslide, e) topples, f) complex landslide and g) rock fall.

the slope exposure in relation to precipitation and wind in one hand, in other hand by the fractures orientation. The slope aspect direction measured from 0 to 360°. Using DEM and GIS allowed extracting the slope direction value, which classified into eight directions (Flat, N, NE, E, SE, S, SW and NW) (Figure 8b).

3.2.3. Lithology

The type of the terrain is one of the most causative parameters for landslide process; the mechanical characteristics of the soil represent the basic data imposed by their type and their history. The significant lithological variation, in the same geological formation can be influenced on the slope movements' distribution. The lithological map of the study area is established by the digitization of the lithological formations of the Saint Denis de sig 1:50,000 scale geological map. According to the lithological characteristics (Table 1), the lithological map is established by the classification of the outcropped lithological formations into five units (Figure 8c).

3.2.4. Distance To Faults

Areas located proximity to faults zones are heavily fractured and present zone of weakness, which provide a geological condition for landslides to occur. In this study, the Euclidian distance was applied to generate the fault buffer zone map and then reclassified into six classes with 500 m of interval < 500, 500-1000, 1000-1500, 1500-2000, 2000-2500 and > 2500 m (Figure 8d).

3.2.5. Lineaments Density

The density map represents the number of lineaments by the area (number / km²). The lineament density indicates the rock fracturing degree. In this study, the lineaments are extracted by the treatment of the Hillshade images produced by the DEM. As a result, the lineament density varies from 0 and 6, their classification into five classes allowed us to produce the lineament density map of the study area (Figure 8e).

3.2.6. Precipitation

Represent all the meteoric water which fall on the earth' surface in liquid or solid form, the precipitation volume participates in the landslides triggering.

Areas with heavy rainfall are more susceptible to the landslides. The average annual precipitation map of the study area is generated from the North Algeria precipitation map (ANRH, 2007). They classified into four zones 250, 300, 350, 400 mm / year (Figure 8f).

3.2.7. Distance to Streams

The proximity to the streams increases the degree of the susceptibility due to erosion caused by the water current in the foot of the talus. The distance to the streams map realized by the buffer zone of the hydrographic network which is classified into five classes (0 - 100, 100 - 200, 200 - 300, 300 - 400, 400 – 500 and >500m) (Figure 8g).

Table 1- Description of the lithological formations outcropped in the study area.

Symbol	Age	Type of formation	Classes	
a	Actual	Major rivers bed formation	Class 5	
qa	Quaternary	Clay-silt alluvium	Class 1	
qec		Limestone	Class 1	
qp		Accumulation glacis	Class 4	
qr		Level of rivers rebuffed terrace	Class 4	
qs		El Habra plain halipeds	Class 1	
qv		Oued Sig polygenic glacis	Class 5	
qlb		Diversifying crusts	Class 5	
qlf		Scree slopes	Class 4	
qlt		Limestone shell	Class 1	
qc		Limestone shell	Class 1	
p		Pliocene	Sandstone and marine sandy marl	Class 5
pc			Sandy marl and red conglomerate	Class 5
ma	Miocene	Gypsum and gypsum marl	Class 4	
mb		Fine sand	Class 5	
mc		Limestone (gypsum series)	Class 1	
md		Marly-limestone	Class 4	
mg		Sand, sandstone and conglomerate	Class 4	
ml		Lithothamniac limestone	Class 2	
mm		Blue marl	Class 4	
mr		Silt and red conglomerate	Class 4	
ms		Sandy marls	Class 5	
mt		Tripoli and tripoli marl	Class 4	
c5_4	Cretaceous	Marly-limestone	Class 3	
c8_7		Marly-limestone	Class 3	

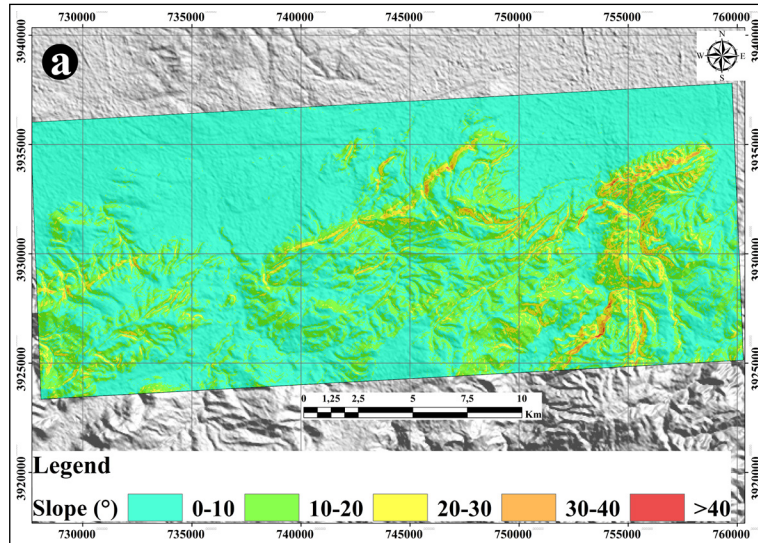


Figure 8- Landslide conditioning factors included in the landslide susceptibility process; a) slope degree, b) aspect, c) lithology, d) distance to faults, e) lineaments density, f) precipitation, g) proximity to the streams, h) land use, i) altitude.

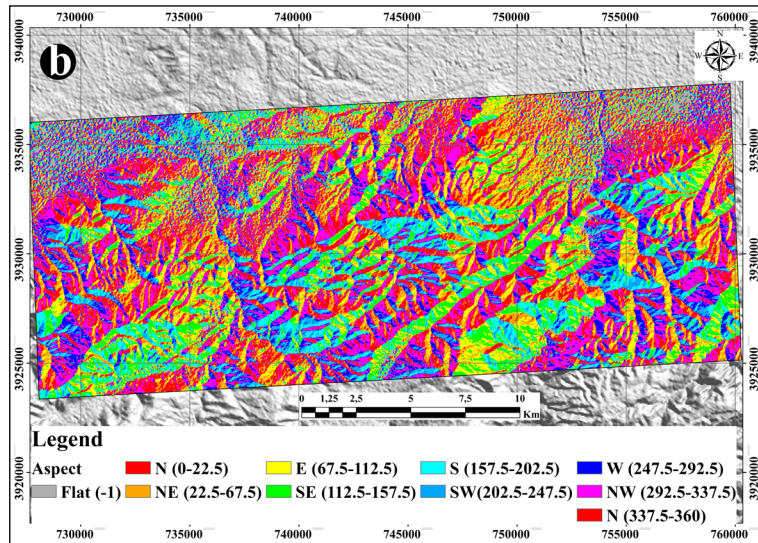


Figure 8- (Continue).

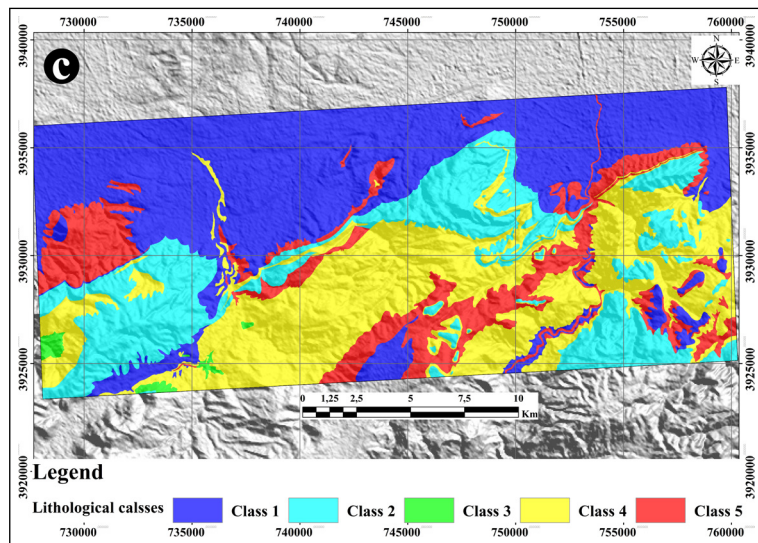


Figure 8- (Continue).

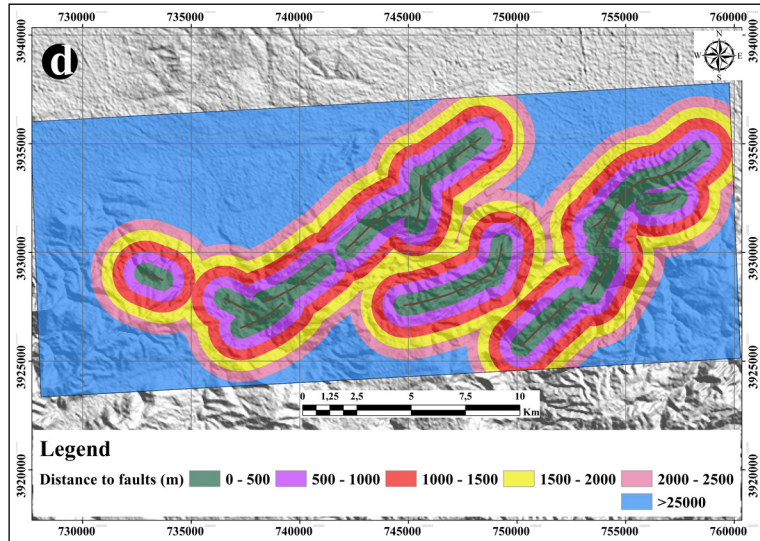


Figure 8- (Continue).

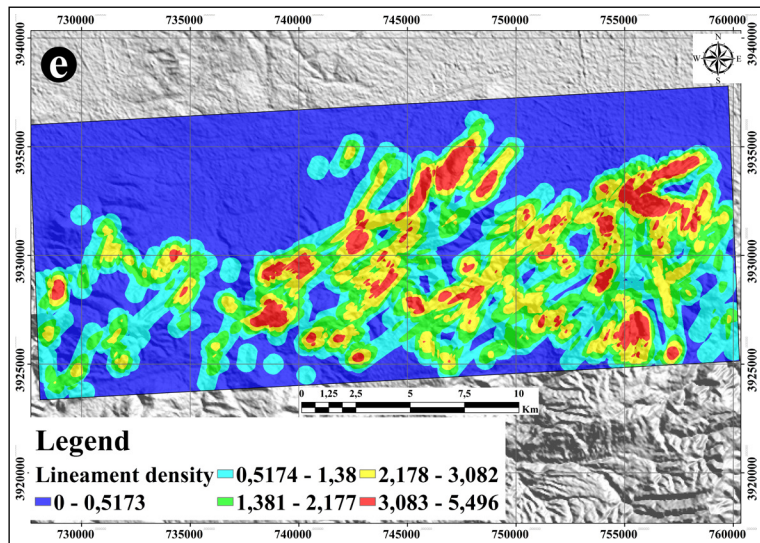


Figure 8- (Continue).

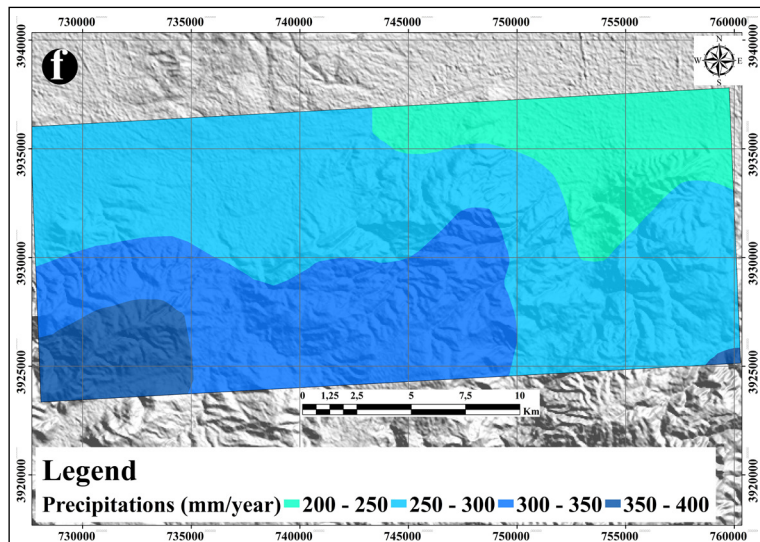


Figure 8- (Continue).

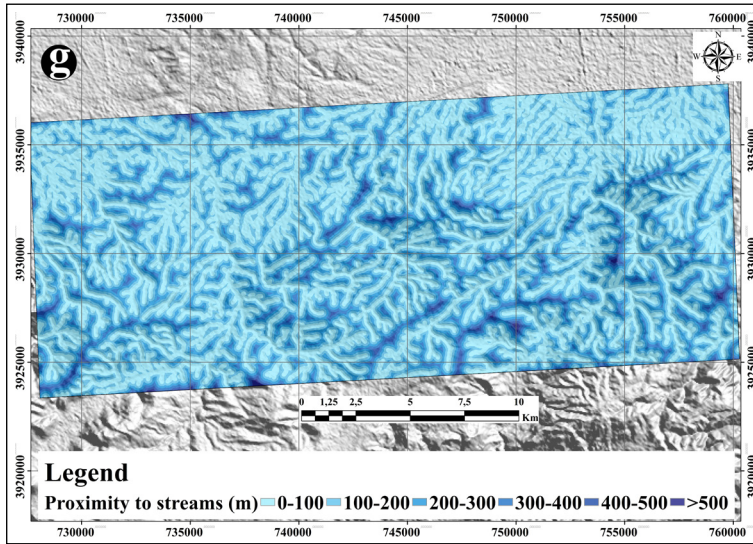


Figure 8- (Continue).

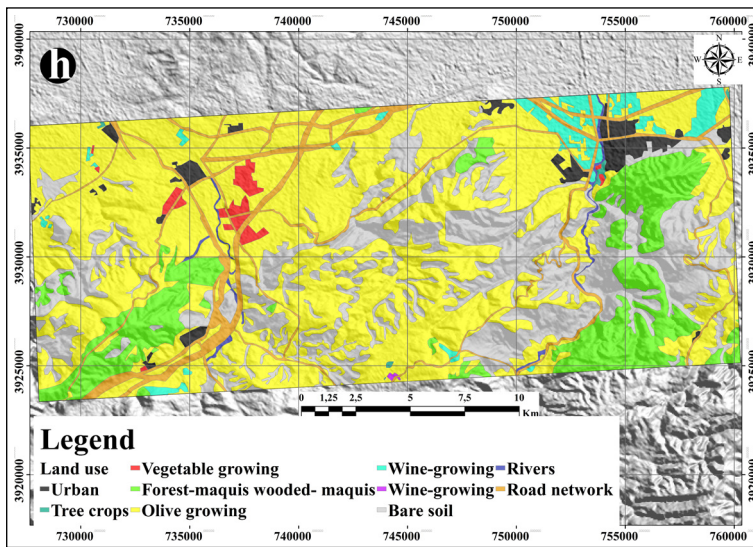


Figure 8- (Continue).

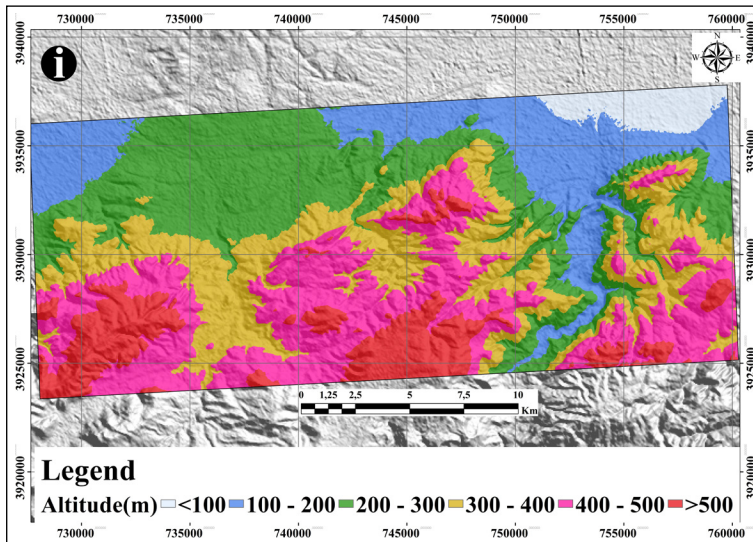


Figure 8- (Continue).

3.2.8. Land Use

The land use type plays a very important role in the slope stability, where the forested area are the least prone to landslide compared to region with no vegetation. In this context, the land use map is established by the digitalization of three 1/25000 scale land use maps (Beneder, 2011), the produced map contain eleven classes (Figure 8h).

3.2.9. Altitude

The altitude is the vertical elevation of a place from the sea level. It is a very important factor which effect land sliding by the fact that difference of several parameters between the different altitude levels as temperature, precipitation and the intensity of the gravity which varies according to the altitude. The altitude map of the study area generated by the classification of the DEM value into six classes: <100, 100-200, 200-300, 300,400, 400-500 and >500 (Figure 8i).

3.3. Analytical Hierarchy Process Method

The AHP method is a multicriteria decision making approach. It is based in complex calculation using matrix algebra formulation. It was developed by Saaty, 1980. This model has been used in several domains, such concerning: The planning of the combined transportations, the rationing of the energy, the risks management, the comparative analysis of the logistic operations, flood hazard and landslide susceptibility.

The AHP model consists to apply the following steps: i) establishment decision making problem into hierarchy, ii) establishment of comparative

judgment, iii) synthesis of priorities and estimating of consistency.

In literature, several studies were based on AHP model to evaluate the weight of the landslide conditioning factors but not for the different classes of the landslide conditioning factors such as the of work of (Barredo et al., 2000; Akgün and Türk, 2010; Mondal and Maiti, 2012). Other researchers used AHP model to calculate the weight of landslide conditioning factors and their different classes, (Intarawichian and Dasananda, 2010; Yalcin et al., 2011; Phukon et al., 2012; Chen et al., 2016). In this research, the AHP technique was used to calculate the weights for each landslide conditioning factors.

In AHP model, to compute the weight of each factor a pair - wise comparison matrix should be established; this is done by comparing each factor against others factors using a value between 1 and 9 or 1/2 and 1/9 according to the effectiveness degree (Table 2).

These judgments are confirmed using consistency ratio, is defined as CR (Equation 1) Saaty, 1977.

$$CR = \frac{CI}{RI} \tag{1}$$

Where RI is the average of the resulting consistency index depending on the order of the matrix given by Saaty, 1980 and CI is the consistency index expressed as:

$$CI = \frac{\lambda_{max} - n}{(n-1)} \tag{2}$$

Where λ_{max} is the largest or principal eigenvalue of the matrix and that can be easily calculated from the matrix and n is the order of the matrix. If CR is greater than 0.1, the comparison matrix is inconsistent and should be revised

Table 2- Scale of preference between two parameters in AHP (Saaty, 1977).

Scales	Degree of preferences	Explanation
1	Equally	Two activities contribute equally to the objective.
3	Moderately	Experience and judgment slightly to moderately favor one activity over another.
5	Strongly	Experience and judgment strongly or essentially favor one activity over another.
7	Very strongly	An activity is strongly favored over another and its dominance is showed in practice.
9	Extremely	The evidence of favoring one activity over another is of the highest degree possible of an affirmation.
2, 4, 6, 8	Intermediate values	Used to represent compromises between the preferences in weights 1, 3, 5, 7 and 9.
Reciprocals	Opposites	Used for inverse comparison.

Table 3 indicates that for the present case the CR value is less than 0.1, which demonstrate that the preferences used to elaborate the comparison matrix, are reasonable. The weight values of each the conditioning factors are defined and calculated by the establishment of the AHP model (Table 3).

Finally, the LSM was constructed using AHP model by the following equation:

$$LSI = \sum_{j=1}^n W_j w_{ij} \tag{3}$$

Where W_j is the weight value of each conditioning factors, w_{ij} is the weight value of class i of causative factor j , and n is the number of the conditioning factors included in the landslide susceptibility process.

For the weighting value of each class (w_{ij}) we attribute of each class a rank varies from 1 to 9 according to the susceptibility degree, Table 4 summarized the calculation results in this study.

3.4. Weight of Evidence Method

The WOE method is one of the most bivariate Bayesian statistical methods used in earth sciences, this method was applied in several domains such as identification of mineral potential (Bonham-Carter, 1989), landslide susceptibility (Regmi et al., 2010) and flood susceptibility (Tehrany et al., 2014; Khosravi et al., 2016). Weight of each landslide conditioning factors can be estimated by combining each conditioning factor with landslide inventory

(presence or absence of landslide, following Equation 4, 5 and 6 (Bonham-Carter, 1994)):

$$W^+ = \ln \frac{P(L^+|B)}{P(L^+|\bar{B})} \tag{4}$$

$$W^- = \ln \frac{P(L^-|B)}{P(L^-|\bar{B})} \tag{5}$$

Where, P is the probability, B and \bar{B} are respectively the presence or absence of potential landslide predictive factor, L and \bar{L} are respectively the presence or absence of landslide. W^+ and W^- are the weight of presence or absence of landslide.

$$WC = W^+ - W^- \tag{6}$$

Where, WC is the weight contrast; indicate the correlation between landslide occurrence and landslide conditioning factors.

Positive and negative values of the weight contrast WC , which mean that the highest value, indicate a great correlation between predictable variable and landslide and vice versa.

The intersection between different causative factors and landslide inventory map (training data) allowed us to extract a database contain landslide area in each class, stable area in each class, total of landslide area and total of stable area. Their statistical analysis allowed estimates W^+ , W^- and WC using Equation 4, 5 and 6, respectively (Table 5). Landslide susceptibility index were assigned by integrate equation in map algebra function in ArcGIS:

Table 3- The pair - wise comparison matrix, factor weights and consistency ratio, slope [1], aspect [2], lithology [3], distance to faults [4], lineaments density [5], precipitation [6], proximity to streams [7], land use [8], altitude [9].

Parameter	[1]	[2]	[3]	[4]	[5]	[6]	[7]	[8]	[9]	Weight
[1]	1	4	2	3	5	3	2	6	7	27.662
[2]	1/4	1	1/3	1/2	1	1/2	1/3	2	4	06.574
[3]	1/2	3	1	2	3	2	1	4	3	16.228
[4]	1/3	2	1/2	1	2	1	1/2	2	3	09.532
[5]	0,2	1	1/3	1/2	1	1/2	1/3	2	3	06.104
[6]	1/3	2	1/2	1	2	1	1/2	2	4	09.851
[7]	1/2	3	1	2	3	2	1	4	5	16.867
[8]	1/6	1/2	1/4	1/2	1/2	1/2	1/4	1	2	4.237
[9]	1/7	1/4	1/3	1/3	1/3	1/4	0,2	1/2	1	2.943
CR = 0.018										$\sum(W) = 100$

Table 4- Rank, and normalized Rank of each class, AHP weighting of each parameter and general weighting of each class.

Parameters	Class	Rank	Normalized rank _(wi)	W _(AHP)	Weighting
Slope (°)	<10	1	0.040	27.662	1.106
	10-20	3	0.120	27.662	3.319
	20-30	5	0.200	27.662	5.532
	30-40	7	0.280	27.662	7.745
	>40	9	0.360	27.662	9.958
Aspect	Flat	1	0.025	6.574	0.164
	N	5	0.128	6.574	0.841
	NE	3	0.076	6.574	0.500
	E	2	0.051	6.574	0.335
	SE	2	0.051	6.574	0.335
	S	5	0.128	6.574	0.841
	SW	6	0.153	6.574	1.006
	W	7	0.179	6.574	1.177
Lithology	Class 1	2	0.076	16.228	1.233
	Class 2	3	0.115	16.228	1.866
	Class 3	5	0.192	16.228	3.116
	Class 4	7	0.269	16.228	4.365
	Class 5	9	0.346	16.228	5.615
Distance to faults (m)	0-500	9	0.333	9.532	3.177
	500-1000	7	0.259	9.532	2.471
	1000-1500	5	0.185	9.532	1.765
	1500-2000	3	0.111	9.532	1.059
	2000-2500	2	0.074	9.532	0.706
	>2500	1	0.037	9.532	0.353
Lineaments density (n/km ²)	0 – 0.51	1	0.047	6.104	0.287
	0.51 – 1.38	2	0.095	6.104	0.580
	1.38 – 2.17	4	0.190	6.104	1.160
	2.17 – 3.08	6	0.285	6.104	1.740
	3.08 – 5.49	8	0.380	6.104	2.320
Precipitation (mm/year)	<250	1	0.090	9.851	0.887
	250-300	2	0.181	9.851	1.783
	300-350	3	0.272	9.851	2.679
	>350	5	0.454	9.851	4.472
Distance to streams (m)	<100	8	0.333	16.867	5.617
	100 – 200	6	0.250	16.867	4.217
	200 – 300	4	0.166	16.867	2.800
	300 – 400	3	0.125	16.867	2.108
	400 – 500	2	0.083	16.867	1.400
	>500	1	0.041	16.867	0.692
Land use	Urban	4	0.108	4.237	0.458
	Tree crops	1	0.027	4.237	0.114
	Vegetable growing	3	0.081	4.237	0.343
	Forest-maquis wooded- maquis	1	0.027	4.237	0.114
	Big culture	4	0.108	4.237	0.458
	Olive growing	1	0.027	4.237	0.114
	Wine-growing	2	0.054	4.237	0.229
	Bare soil	8	0.216	4.237	0.915
	Rivers	7	0.189	4.237	0.801
	Road network	6	0.162	4.237	0.686
Altitude (m)	<100	1	0.035	2.943	0.103
	100 – 200	2	0.071	2.943	0.209
	200 – 300	4	0.142	2.943	0.418
	300 – 400	6	0.214	2.943	0.630
	400 – 500	7	0.250	2.943	0.736
	>500	8	0.285	2.943	0.839

Table 5- Statistical analysis of the WOE parameters and weight of each conditioning factor.

Parameter	Class	Pixels in	Landslide pixels classes	W+	W-	C
		the classes				
Slope (°)	0 – 10	1759734	2075	-0.9979085	0.8379506	-1.8358591
	10-20	706082	4877	0.77546774	-0.56545143	1.34091918
	20 – 30	132384	1103	0.96436012	-0.09014597	1.05450609
	30 - 40	13289	245	1.76884112	-0.0248005	1.79364162
	> 40	436	38	3.3948006	-0.00441496	3.39921556
Aspect	Plat	59886	6	-3.46458842	0.02254948	-3.48713791
	N	448266	1468	0.02559732	-0.00538576	0.03098308
	NE	365636	813	-0.36263845	0.04837752	-0.41101597
	E	303316	1153	0.1752127	-0.02546451	0.20067721
	SE	286127	1726	0.63927771	-0.11626756	0.75554527
	S	218225	686	-0.01545604	0.00139737	-0.0168534
	SW	200455	408	-1.50799814	0.06288188	-1.57088002
	W	261235	1936	-0.7164873	0.05538602	-0.77187332
NW	468779	142	0.25847951	-0.0666118	0.32509131	
Lithology	Class 1	998012	0	0	0	0
	Class 2	504972	332	-1.57795563	0.1746274	-1.75258303
	Class 3	15538	0	0	0	0
	Class 4	751227	6541	1.01363738	-1.21505342	2.2286908
	Class 5	342175	1426	0.27223717	-0.04826394	0.32050111
Distance to Fault (m)	0-500	282420	921	-2.3402519	0.51924938	-2.85950130
	500-1000	303698	1967	0.30942590	-0.3997504	0.34940095
	1000-1500	330899	1936	0.70227021	-0.1532889	0.85555911
	1500-2000	320918	2061	0.60850033	-0.1291375	0.73763786
	2000-2500	255011	1108	0.71079527	-0.1458925	0.85668780
>25000	1118978	345	-0.9965183	-0.0026253	-0.95789279	
Lineaments density (km/km ²)	0 - 0.51	1185867	223	-2.83480325	0.58057402	-3.41537727
	0.51 - 1.38	514074	2063	0.22963675	-0.06527754	0.29491429
	1.38 - 2.17	427344	2832	0.54645869	-0.23699526	0.78345395
	2.17 - 3.08	340810	2265	0.73673936	-0.1776738	0.91441316
	3.08 - 5.49	143829	955	0.73581456	-0.06520433	0.8010189
Distance to Streams (m)	0 - 100	1187425	5344	0.34476434	-0.42279188	0.76755622
	100 - 200	827835	2281	-0.14761911	-0.14103651	-0.00658259
	200 - 300	426302	521	-0.96210874	0.11404971	-1.07615845
	300 - 400	141918	189	-0.87610342	0.03304562	-0.90914905
	400- 500	25403	3	-3.30007054	0.00944381	-3.30951435
Precipitation (mm/year)	250	409260	255	-1.63639749	0.1398383	-1.77623579
	300	1311790	169	-0.29222467	0.22800147	-0.52022613
	350	711342	4785	0.74890377	-0.5364303	1.28533409
	400	179532	3129	-1.22344662	0.05090179	-1.27434841
Land use	Urban	58744	0	0	0	0
	Tree crops	2891	0	0	0	0
	Vegetable growing	713	0	0	0	0
	Forest-maquis wooded- maquis	309301	441	-0.80650041	0.07176416	-0.87826456
	Big culture	1336674	2122	-0.69965686	0.42439734	-1.1240542
	Olive growing	66130	0	0	0	0
	Wine-growing	25103	0	0	0	0
	Bare soil	632357	5493	1.00684737	-0.80267428	1.80952165
	Rivers	13515	0	0	0	0
Road network	167799	282	-0.64290247	-0.03440622	-0.60849624	
Altitude(m)	< 100	81259	0	0	0	0
	100 - 200	408742	474	-1.01479799	0.11206231	-1.1268603
	200 - 300	687331	1993	-0.0960651	0.41126357	-0.50732867
	300 - 400	544439	2612	0.40886173	-0.0629098	0.4717716
	400 - 500	608334	2924	0.41099391	-0.1672183	0.57821221
	>500	281820	334	-0.99234467	0.0734715	-1.06581618

$$LSI_{woc} = Wc * Slope + Wc * Aspect + Wc * Lithology + Wc * Distance\ to\ faults + Wc * Lineaments\ density + Wc * Precipitation + Wc * Distance\ to\ streams + Wc * Land\ use + Wc * Altitude \quad (7)$$

3.5. The Logistic Regression Method

Logistic regression is one of the most widely used statistical methods in geosciences. The method is based on the relationships established between the values of certain quantitative or qualitative variables and the presence or absence of a certain phenomenon. For landslides, it allows to determine the relative contributions of the different causes, also benefiting from the graphical expression of the prediction model. One of the most important advantages of this method is that the independent variables can have both continuous and discrete values, occurring in any combination of the two types. Also, compared to other statistical methods, it does not require a normal distribution of values. The probability (P) of landslide occurrence, calculated for each elementary surface unit, can take values between 0 and 1, according to the Equation 8:

$$P(y) = \frac{1}{1 + e^{-y}} \quad (8)$$

Where, P(y) varies from 0 to 1, Y is expressed by the following linear equation

$$Y = b_0 + b_1x_1 + b_2x_2 + \dots + b_nx_n \quad (9)$$

Where, Y is the dependent variable presented by the absence (0) or presence (1) of a phenomenon, b_0 is the intercept, b_1, b_2, \dots, b_n are the partial regression coefficients, x_1, x_2, \dots, x_n are the independent variables (predisposing factors).

In this study, a data base contains the raster landslide and the conditioning factors maps created by the combine module in ArcGIS software and converted in dbf format. For the analysis process, the correlation between the landslide distribution and each causative factor are calculated using Xlstat package, in order to produce a LSM. For each conditioning factor class, the ratio between the landslide percentage and the percentage of the same class is used to estimate the

weight of each class (Table 6). A quantitative value from 0 to 1 is given as weight factor for each class.

For this study, the logistic regression model established is given in following equation:

$$P(y) = 1 / (1 + \exp(-(-8,18464 - 0,12674 * Fault + 0,14324 * Precipitation + 0,25625 * Lineament\ Density - 0,69206 * Distance\ to\ streams + 0,23182 * Land\ use + 0,22328 * Slope + 0,52545 * Lithology - 0,00363 * Aspect + 0,13794 * Altitude))) \quad (10)$$

4. Results and Discussion

The obtained pair wise comparison matrix (Table 4) showed the most influenced parameters to the landslide is the slope with a weighting of 0.228 as well as the lithology and the distance to the streams. The least influenced parameters for the landslide occurrence are the land use and the Altitude.

The outcome of this analysis indicates that the LSI increase with the slope degree increasing. Aspect analysis indicates that north, south, western and north western slope directions of the reliefs are the most susceptible by the landslide. The major rivers bed formation, clay-silt alluvium, accumulation glacia, the river Sig polygenic glacia, sandy marls, fine sand, sandy marl and red conglomerate, sandstone and marine sandy marl, scree slopes and diversifying crusts present the most susceptible outcropping formations to landslides. Areas located near faulting zone present the most susceptible zone to the landslides. The outcropped lithological formations characterized by high lineaments density represent the weakness areas which are the most landslide prone areas. The landslides are directly related to the precipitations, in this area the landslide susceptibility increase with the precipitation increasing, the most prone areas that are characterized by heavy rainfall. We mentioned that areas located near the streams characterized by the high and very high susceptibility where the important flow velocity erodes the lower part of the talus. The areas that are characterized by high density of vegetation like forest lands, scrublands provide hydrological and mechanical effects that typically stabilize slopes with considered as the less landslide susceptible areas, in this area the barren land, the rivers zone and road network areas considered as the most landslide prone areas where the slope stability effects are absent. In

Table 6- Statistical analysis of the LR model and weight of each conditioning factor.

Parameters	Class	Pixels in classes	Landslide pixels classes	% of total area	% of landslide area	Factor weight	LR	LR weighting
Slope (°)	<10	1759734	2075	67.373068	24.886064	0.42546648	0.22383	0.095232161
	10-20	706082	4877	27.033012	58.491245	1		0.22383
	20-30	132384	1103	5.068446	13.228592	0.22616363		0.050622204
	30-40	13289	245	0.508782	02.938355	0.0502358		0.011244279
	>40	436	38	0.016693	0.455745	0.00779168		0.001744011
Aspect	Flat	59886	6	2.292792	0.07196	0.00309917	-0.00363	-0.00001125
	N	448266	1468	17.162285	17.606141	0.75826446		-0.0027525
	NE	365636	813	13.998717	9.75054	0.41993802		-0.00152438
	E	303316	1153	11.612738	13.828256	0.59555785		-0.00216188
	SE	286127	1726	10.954641	20.700408	0.89152893		-0.00323625
	S	218225	686	8.354949	8.227393	0.35433884		-0.00128625
	SW	200455	142	7.674608	1.703046	0.07334711		-0.00026625
	W	261235	408	10.001627	4.89326	0.2107438		-0.000765
Lithology	Class 1	998012	0	38.209826	0	0	0.52545	0
	Class 2	504972	332	19.333327	3.98177	0.05075677		0.026670142
	Class 3	15538	0	0.594887	0	0		0
	Class 4	751227	6541	28.761431	78.448069	1		0.52545
	Class 5	342175	1460	13.100491	17.510194	0.22320746		0.11728436
Distance to faults (m)	0-500	1118633	921	42.827914	11.045814	0.44687045	-0.12674	-0.05663636
	500-1000	253903	1967	9.720915	23.590789	0.95439107		-0.12095952
	1000-1500	318857	1936	12.20774	23.218997	0.93934983		-0.1190532
	1500-2000	328963	2061	12.594657	24.718158	1		-0.12674
	2000-2500	301731	1108	11.552055	13.288558	0.53760311		-0.06813582
	>25000	281499	345	10.777453	4.137683	0.16739447		-0.02121557
Lineaments density (n/km ²)	0 – 0.51	1185867	223	45.402031	2.674502	0.07874294	0.25625	0.020177878
	0.51 – 1.38	514074	2063	19.681806	24.742144	0.72846045		0.186667991
	1.38 – 2.17	427344	2832	16.361266	33.96498	1		0.25625
	2.17 – 3.08	340810	2265	13.048231	27.164788	0.79978814		0.20494571
	3.08 – 5.49	143829	955	5.506628	11.453586	0.33721751		0.086411988
Precipitation (mm/year)	<250	409260	255	15.668903	3.058287	0.05329154	0.14324	0.00763348
	250-300	179532	169	6.873551	2.026865	0.0353187		0.005059051
	300-350	711342	4785	27.234396	57.387863	1		0.14324
	>350	1311790	3129	50.223111	37.526985	0.6539185		0.093667285
Distance to streams (m)	<100	1187425	5344	45.461681	64.092108	1	-0.69206	-0.69206
	100 – 200	827835	2281	31.69444	27.35668	0.42683383		-0.29539462
	200 – 300	426302	521	16.321372	6.248501	0.09749251		-0.06747067
	300 – 400	141918	189	5.433464	2.266731	0.03536677		-0.02447592
	400 – 500	25403	3	0.972578	0.03598	0.00056138		-0.00038851
	>500	3041	0	0.116428	0	0		0
Land use	Urban	66130	0	2.531849	0	0	0.23182	0
	Tree crops	25103	0	0.961092	0	0		0
	Vegetable growing	2891	0	0.110685	0	0		0
	Forest-maquis wooded- maquis	309301	441	11.841879	5.289038	0.080284		0.018611436
	Big culture	1336674	2122	51.175819	25.449748	2.58859566		0.600088247
	Olive growing	13515	0	0.517434	0	0		0
	Wine-growing	713	0	0.027298	0	0		0
	Bare soil	632357	5493	24.210381	65.879108	1		0.23182
	Rivers	167799	282	6.424342	3.382106	0.05133807		0.011901191
Road network	58744	0	2.249069	0	0	0		
Altitude (m)	<100	81259	0	3.111077	0	0	0.13794	0
	100 – 200	408742	474	15.649071	5.684817	0.1621067		0.022360999
	200 – 300	687331	1994	26.315112	23.914608	0.68194254		0.094067155
	300 – 400	544439	2612	20.844358	31.326457	0.89329685		0.123221368
	400 – 500	608334	2924	23.290638	35.068362	1		0.13794
	>500	281820	334	10.789743	4.005757	0.11422709		0.015756484

this study, the susceptibility to the landslide is increase with the altitude of the reliefs increasing.

The application of the AHP method shows that the global landslide susceptibility index varies between 5.647 and 31.332, their classification into five landslide susceptibility classes using natural break (jenks) shows that 17.87% of the total area characterized by null susceptibility to the landslide, 29.82% of the study area characterized by low susceptibility, 21.24% of the total area characterized by a moderate susceptibility, 20.69% characterized by high susceptibility, the rest of the study area (10.38%) characterized by very high landslide susceptibility (Figure 9a, b).

According to the obtained LSM (Figure 9), the most landslide susceptibility areas are located in the east and the center part of the study area, whereas the northern part of the map characterized by low and null landslide susceptibility.

For the weight of evidence model, the resulting weight contrast, are shown in (Table 5), the

interpretation of this results demonstrate than the more susceptible classes correspond to slope greater than 40°, SE and NW facing slopes, very susceptible lithological formation (class 4), (1000 - 1500) class fault proximity field, rocks characterized by high density of lineament, area with high precipitation (300 - 400), area near streams, barren land, and altitude range between 400 and 500 meters. The values less or equal to zero of C indicate that this class does not affect the distribution of landslide in the Echorfa region.

The final LSI of study area for WOE approach range between -19.1243 and 10.7522. The LSM of the Echorfa region was established by classification of LSI values into five levels (Figure 10a) using natural break method: Null with (27.97%) of total area, Low with 19.08%, Moderate with 20.63%, the High level 20.47%, and 11.85% falls in very high level (Figure 10b).

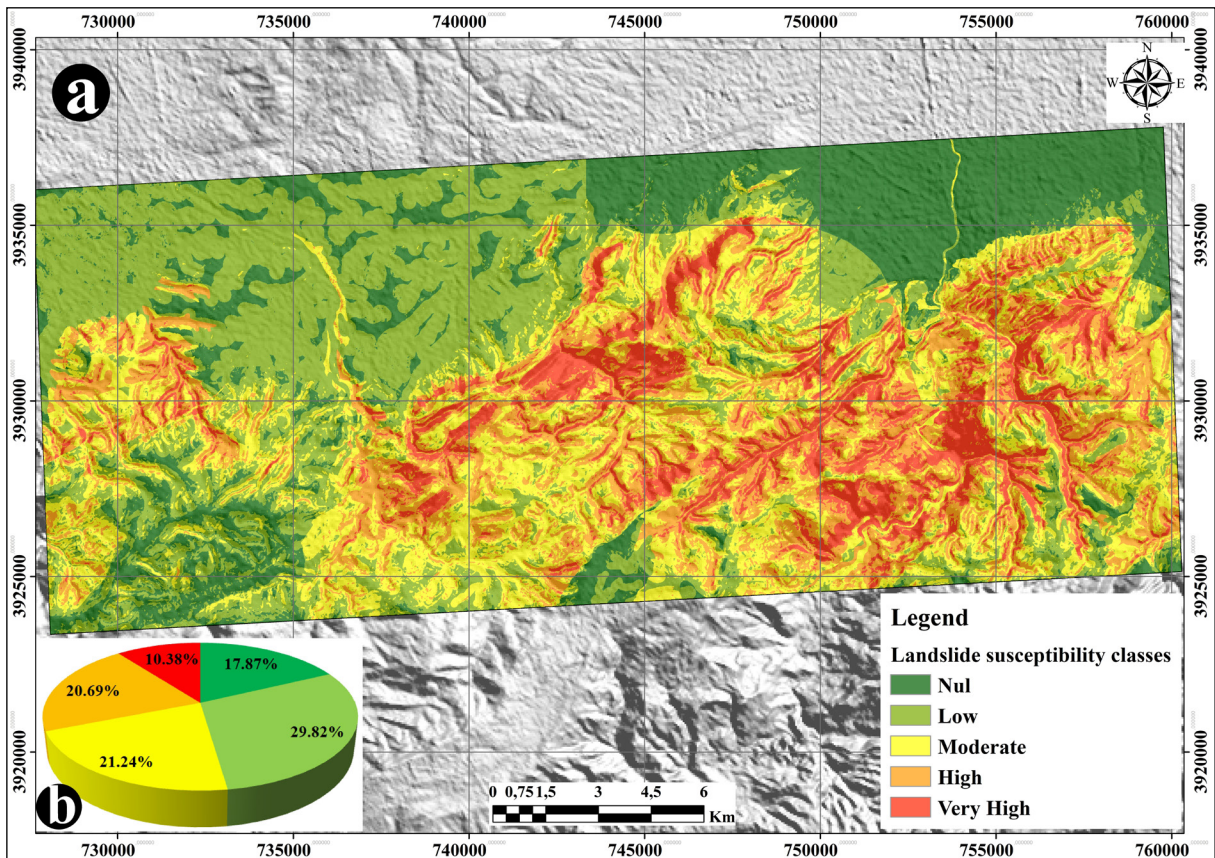


Figure 9- a) The AHP -landslide susceptibility map, b) distribution pie - chart of the landslide susceptibility classes.

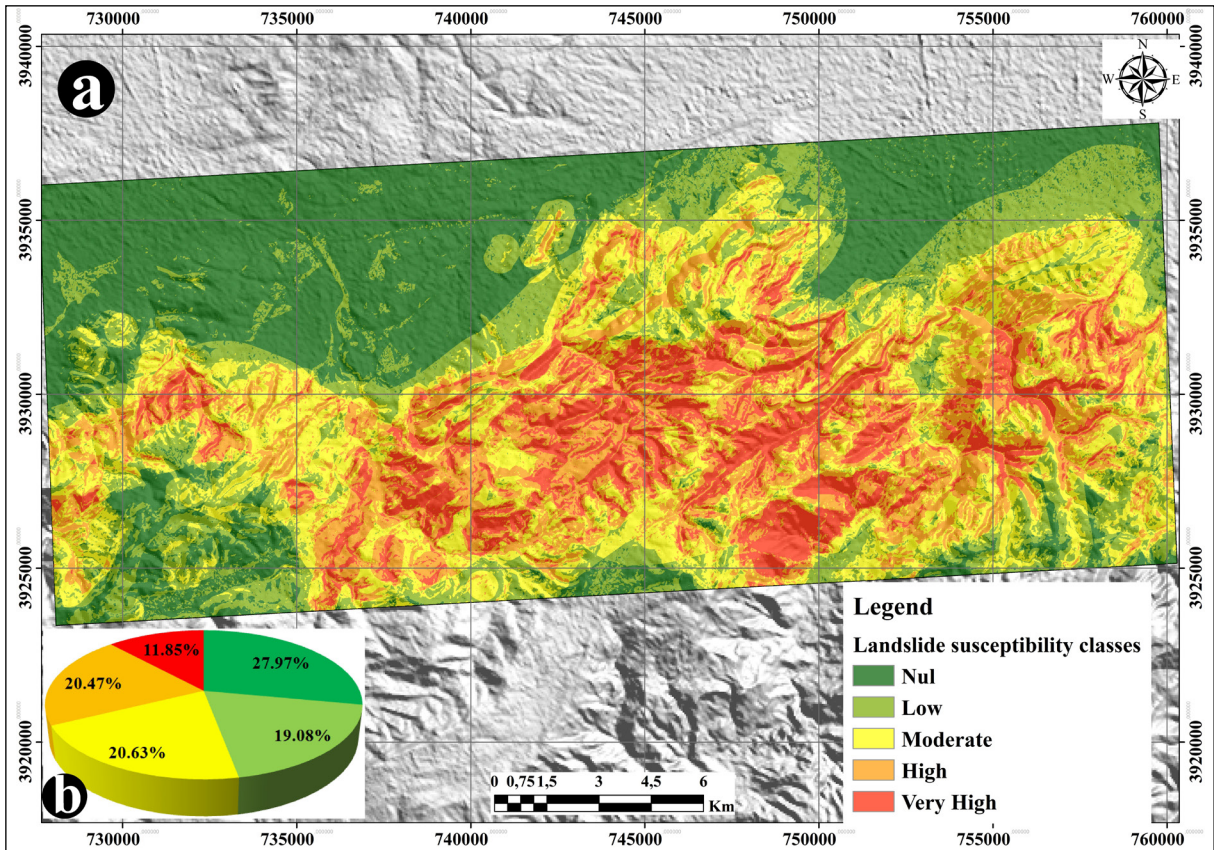


Figure 10–a) The WOE - landslide susceptibility map, b) distribution pie - chart of the landslide susceptibility classes.

For the LR model and according to the Table 6 and Equation 10, slope, lithology, lineaments density, precipitation, land use and altitude give positive values which mean that these factors contribute to occurrence of the landslide. On the other hand, Aspect, distance to fault and proximity to streams has a negative role in landslides occurrence. By using Equation 10, the landslide occurrence probability is estimated. The produced LSM using LR model indicate that 37.64 % of the total area characterized by no susceptibility, 30.52% presented by low susceptibility, 19.15% characterized by moderate susceptibility, 8.75% of the total area falls in high susceptibility and the rest of the study area 3.93% represented by very high susceptibility (Figure 11).

5. Validation

The validation of the obtained LSMs presents an essential step in order to calculate the performance of the used method in landslides prone area zoning. In this context, Roc Curve validation technique is used

to calculate the performance of the statistical models integrated in the landslide susceptibility mapping.

ROC curve method is used to validate the obtained LSMs established by the AHP, WOE and LR methods. This statistic method is based in the comparison of the obtained LSM and the produced inventory map (validation data). The realization of the ROC curve consists first in classifying the LSI into 100 classes with an interval of 1%, then, the reclassified map is combined with the landslide events map, and finally, the production of the ROC curve is based in statistical analysis of the converted combination result file into compatible Excel software format.

To calculate the performance of the used methods, it is generally based on the evaluation of the area under curve (AUC) the ROC curve obtained. The AUC result is 95.13% for the WOE model, 91.92% for the AHP method and 83.57% for the LR model (Figure 12).

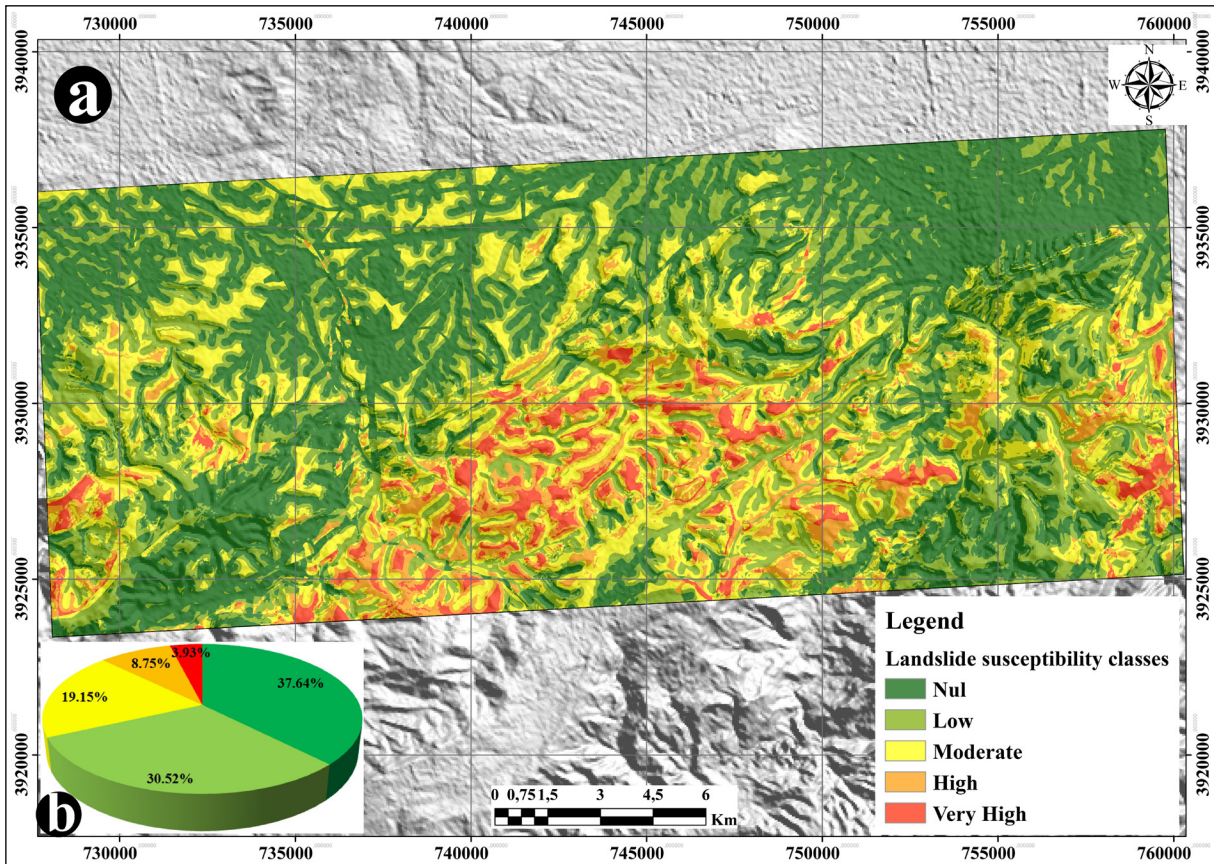


Figure 11– a) The LR - landslide susceptibility map, b) distribution pie - chart of the landslide susceptibility classes.

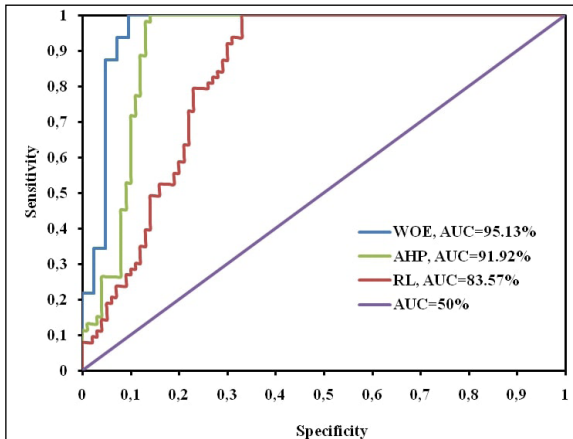


Figure 12- Diagram of ROC curve representing the performance of the statistical models.

ROC curve obtained for WOE, AHP and LR indicate that the used models in this research give good results in LSM. By comparing the ROC curve results we mentioned that the LSM produced by WOE method is the successful one.

6. Conclusion

The landslides presented one of the most common geological hazards in the world; they cause annually a considerable damages and human losses. In Algeria, a few attempts at landslide are applied in the northeastern part of the country. These contributions are generally focused on the application of the geophysical methods for landslide investigations on locale scale and the application of statistical methods based in GIS for the landslide susceptibility zoning on medium scale.

The investigations in the Echorfa region (NW of Algeria) indicate the lake on information about slope movements occurred in this area that involved the production of the landslide prone areas maps.

The LSMs produced by the categories the GSI into five classes according to the susceptibility degree. High and very high susceptibility characterizes the reliefs of the east and central part of the study area. Insignificant and low susceptibility classes

characterizes the northern part of this region (plains and plateaus) constituting the slope movements sheltered zones.

The validation process of the obtained results of the ROC curve model indicates the aptitude of the three models in the landslide susceptibility mapping. Hence, the WOE approach gives reasonable good accuracy in predicting landslide susceptibility of the Echorfa region.

The obtained LMSs can be considered as a basic document for the concerned authorities to take preventive measurements in the high and very high landslide susceptibility zones. In other hand, it provides a useful tool for the land use planner to select suitable fields for the future projects.

References

- Achour, Y., Boumezbeur, A., Hadji, R., Chouabbi, A., Cavaleiro, V., Bendaoud, E. A. 2017. Landslide susceptibility mapping using analytic hierarchy process and information value methods along a highway road section in Constantine, Algeria. *Arabian Journal of Geosciences* 10, 194.
- Akgün, A., Türk, N. 2010. Landslide susceptibility mapping for Ayvalık (Western Turkey) and its vicinity by multicriteria decision analysis. *Environmental Earth Sciences* 61, 595-611.
- ANRH. 2007. Agence Nationale des ressources hydriques. Carte des pluies moyennes annuelles du Nord de l'Algérie, INCT., Alger, Algeria.
- Ayadi, A., Ousadou-Ayadi, F., Bourouis, S., Benhallou, H. 2002. Seismotectonics and seismic quietness of the Oranie region (Western Algeria): The Mascara earthquake of August 18 th 1994, $M_w=5.7$, $M_s=6.0$. *Journal of Seismology* 6, 13-23.
- Baeza, C., Corominas, J. 2001. Assessment of shallow landslide susceptibility by means of multivariate statistical techniques. *Earth Surface Processes and Landforms: The Journal of the British Geomorphological Research Group* 26, 1251-1263.
- Barredo, J., Benavides, A., Hervás, J., van Westen, C. J. 2000. Comparing heuristic landslide hazard assessment techniques using GIS in the Tirajana basin, Gran Canaria Island, Spain. *International Journal of Applied Earth Observation and Geoinformation* 2, 9-23.
- Belayadi, I., Bezzeghoud, M., Nadji, A., Fontiela, J. 2017. Sismicité de l'Algérie Nord Occidentale entre 1790 et 2016: catalogue sismique. *Comunicação Geológicas* 104.
- Beneder, 2011. Carte d'occupation du sol wilaya d'Oran, Mascar et Sidi Belabess notice explicative. Bureau national d'études pour le développement rural, Rapport inédite.
- Benouar, D., Aoudia, A., Maouche, S., Meghraoui, M. 1994. The 18 August 1994 Mascara (Algeria) earthquake-a quick-look report. *Terra Nova* 6, 634-638.
- Bonham-Carter, G. F. 1989. Weights of evidence modeling: a new approach to mapping mineral potential. *Statistical applications in the Earth Sciences* 171-183.
- Bonham-Carter, G. F. 1994. *Geographic Information Systems for Geoscientists Modeling with GIS*. Elsevier, 398.
- Bouhadad, Y., Laouami, N. 2002. Earthquake hazard assessment in the Oran region (Northwest Algeria). *Natural Hazards* 26, 227-243.
- Bourenane, H., Bouhadad, Y., Guettouche, M. S., Braham, M. 2015. GIS-based landslide susceptibility zonation using bivariate statistical and expert approaches in the city of Constantine (Northeast Algeria). *Bulletin of Engineering Geology and the Environment* 74, 337-355.
- Bourenane, H., Guettouche, M. S., Bouhadad, Y., Braham, M. 2016. Landslide hazard mapping in the Constantine city, Northeast Algeria using frequency ratio, weighting factor, logistic regression, weights of evidence, and analytical hierarchy process methods. *Arabian Journal of Geosciences* 9, 154.
- Chen, W., Li W., Chai, H., Hou, E., Li, X., Ding, X. 2016. GIS-based landslide susceptibility mapping using analytical hierarchy process (AHP) and certainty factor (CF) models for the Baozhong region of Baoji City, China. *Environmental Earth Sciences* 75, 63.
- Chen, W., Peng, J., Hong, H., Shahabi, H., Pradhan, B., Liu, J., Zhu, A. X., Pei, X., Duan, Z. I. 2018. Landslide susceptibility modelling using GIS-based machine learning techniques for Chongren County, Jiangxi Province, China. *Science of the Total Environment* 626, 1121-1135.
- Chen, W., Pourghasemi, H. R., Zhao, Z. 2017. A GIS-based comparative study of Dempster-Shafer, logistic regression and artificial neural network models

- for landslide susceptibility mapping. *Geocarto International* 32, 367-385.
- Corominas, J., Van Westen, C., Frattini, P., Cascini, L., Malet, J-P., Fotopoulou, S., Catani, F., Van Den Eeckhaut, M., Mavrouli, O., Agliardi, F., Pitolakis, K., Winter, M-G., Pastor, M., Ferlisi, S., Tofani, V., Herva's, J., Smith, J-T. 2014. Recommendations for the quantitative analysis of landslide risk. *Bulletin of Engineering Geology and the Environment* 73, 209-263.
- Cruden, D. M., Varnes, D. J. 1996. *Landslide Types and Processes*, Special Report, Transportation Research Board, National Academy of Sciences 247, 36-75.
- Dahoua, L., Yakovitch, S., Hadji, R H. 2017. GIS-based technic for roadside-slope stability assessment: an bivariate approach for A1 East-west highway, North Algeria. *Mining Science* 24.
- Djeral, L., Khoudi, I., Alimrina, N., Melbouci, B., Bahar, R. 2017. Assessment and mapping of earthquake-induced landslides in Tizirt City, Algeria. *Natural Hazards* 87, 1859-1879.
- El Mekki, A., Hadji, R., Chemseddine, F. 2017 Use of slope failures inventory and climatic data for landslide susceptibility, vulnerability, and risk mapping in souk Ahras region. *Mining Science* 24.
- Ercanoğlu, M., Gökçeoğlu, C., Van Asch, T. W. 2004. Landslide susceptibility zoning north of Yenice (NW Turkey) by multivariate statistical techniques. *Natural Hazards* 32, 1-23.
- Fell, R., Corominas, J., Bonnard, C., Cascini, L., Leroi, E., Savage, W. Z. 2008. Guidelines for landslide susceptibility, hazard and risk zoning for land-use planning. *Engineering Geology* 102, 99-111.
- Flentje, P. N., Miner, A., Whitt, G., Fell, R. 2007. Guideline for landslide susceptibility, hazard and risk zoning for land use planning. *Australian Geomechanics* 42, 13-36.
- Guemache, M. A., Chatelain, J. L., Machane, D., Benahmed, S., Djadia, L. 2011. Failure of landslide stabilization measures: The Sidi Rached viaduct case (Constantine, Algeria). *Journal of African Earth Sciences* 59, 349-358.
- Guessoum, N., Benhamouche, A. A., Bouhadad, Y., Bourenane, H., Abbouda, M. 2018. Field evidence of Quaternary seismites in the Mostaganem-Relizane (western Algeria) region: Seismotectonic implication. *Arabian Journal of Geosciences* 11, 641.
- Hadji, R., Rais, K., Gadri, L., Chouabi, A., Hamed, Y. 2017. Slope failure characteristics and slope movement susceptibility assessment using GIS in a medium scale: a case study from Ouled Driss and Machroha municipalities, Northeast Algeria. *Arabian Journal for Science and Engineering* 42, 281-300.
- Hallal, N., Yelles Chaouche, A., Hamai, L., Lamali, A., Dubois, L., Mohammedi, Y., Hamidatou, M., Djadia, L., Abtout, A. 2019. Spatiotemporal evolution of the El Biar landslide (Algiers): new field observation data constrained by ground-penetrating radar investigations. *Bulletin of Engineering Geology and the Environment* 78(3).
- Intarawichian, N., Dasananda, S. 2010. Analytical hierarchy process for landslide susceptibility mapping in lower Mae Chaem watershed, Northern Thailand. *Suranaree Journal of Science and Technology* 17.
- Karim, Z., Hadji, R., Hamed, Y. 2019. GIS-based approaches for the landslide susceptibility prediction in Setif Region (NE Algeria). *Geotechnical and Geological Engineering* 37, 359-374
- Khosravi, K., Nohani, E., Maroufinia, E., Pourghasemi, H. R. 2016. A GIS-based flood susceptibility assessment and its mapping in Iran: a comparison between frequency ratio and weights-of-evidence bivariate statistical models with multi-criteria decision-making technique. *Natural Hazards* 83, 947-987.
- Lee, S., Ryu, J. H., Won, J. S., Park, H. J. 2004. Determination and application of the weights for landslide susceptibility mapping using an artificial neural network. *Engineering Geology* 71, 289-302.
- Mahdadi, F., Boumezbeur, A., Hadji, R., Kanungo, D. P., Zahri, F. 2018. GIS-based landslide susceptibility assessment using statistical models: a case study from Souk Ahras province, NE Algeria. *Arabian Journal of Geosciences* 11, 476.
- Marinas, J. L., Salord, R. 1991. Problems regarding the investigation of the 1790 oran seismic period. *Tectonophysics* 193, 237-239.
- Merghadi, A., Abderrahmane, B., Tien Bui, D. 2018. Landslide susceptibility assessment at Mila Basin (Algeria): a comparative assessment of prediction capability of advanced machine learning methods. *ISPRS International Journal of Geo-Information* 7, 268.
- Micheletti, N., Foresti, L., Robert, S., Leuenberger, M., Pedrazzini, A., Jaboyedoff, M., Kanevski, M. 2014. Machine learning feature selection

- methods for landslide susceptibility mapping. *Mathematical Geosciences* 46, 33-57
- Mohammady, M., Pourghasemi, H. R., Pradhan, B. 2012. Landslide susceptibility mapping at Golestan Province, Iran: a comparison between frequency ratio, Dempster–Shafer, and weights-of-evidence models. *Journal of Asian Earth Sciences* 61, 221-236.
- Mondal, S., Maiti, R. 2012. Landslide susceptibility analysis of Shiv-Khola watershed, Darjiling: a remote sensing and GIS based Analytical Hierarchy Process (AHP). *Journal of the Indian Society of Remote Sensing* 40, 483-496.
- Pham, B. T., Bui, D. T., Prakash, I., Dholakia, M. 2017. Hybrid integration of Multilayer Perceptron Neural Networks and machine learning ensembles for landslide susceptibility assessment at Himalayan area (India) using GIS. *Catena* 149, 52-63.
- Phukon, P., Chetia, D., Das, P. 2012. Landslide susceptibility assessment in the Guwahati city, Assam using analytic hierarchy process (AHP) and geographic information system (GIS). *International Journal of Computer Applications in Engineering Sciences* 2, 1-6.
- Regmi, N. R., Giardino, J. R., Vitek, J. D. 2010. Modeling susceptibility to landslides using the weight of evidence approach: Western Colorado, USA. *Geomorphology* 115, 172-187.
- Roukh, Z. 2020. Cartographie algébrique d'aléa multirisque du littoral Oranie, Nord Ouest de l'Algérie, (risque sismique, glissement de terrain, inondation). Thèse de doctorat, Université d'Oran 2, 289.
- Saaty, T. L. 1977. A scaling method for priorities in hierarchical structures. *Journal of Mathematical Psychology* 15, 234-281
- Saaty, T. L. 1980. *The Analytic Hierarchy Process: Planning, Priority Setting, Resource Allocation*, MacGraw-Hill, New York, International Book Company, 287.
- Santacana, N., Baeza, B., Corominas, J., De Paz, A., Marturiá, J. 2003. A GIS-based multivariate statistical analysis for shallow landslide susceptibility mapping in La Pobla de Lillet area (Eastern Pyrenees, Spain). *Natural Hazards* 30, 281-295.
- Süzen, M. L., Doyuran, V. 2004. Data driven bivariate landslide susceptibility assessment using geographical information systems: a method and application to Asarsuyu catchment, Turkey. *Engineering Geology* 71, 303-321.
- Tehrany, M. S., Pradhan, B., Jebur, M. N. 2014. Flood susceptibility mapping using a novel ensemble weights-of-evidence and support vector machine models in GIS. *Journal of Hydrology* 512, 332-343.
- Thomas, G. 1985. Géodynamique d'un bassin intramontagneux Le bassin du Bas Chélif occidental (Algérie) durant le Mio-Plio-Quaternaire. Thèse de doctorat, Université de Pau, 594.
- Xu, C., Xu, X., Dai, F., Saraf, A. K. 2012. Comparison of different models for susceptibility mapping of earthquake triggered landslides related with the 2008 Wenchuan earthquake in China. *Computers and Geosciences* 46, 317-329.
- Yalçın, A., Reis, S., Aydınöglü, A., Yomraloğlu, T. 2011. A GIS-based comparative study of frequency ratio, analytical hierarchy process, bivariate statistics and logistics regression methods for landslide susceptibility mapping in Trabzon, NE Turkey. *Catena* 85, 274-287.
- Yılmaz, I. 2009. Landslide susceptibility mapping using frequency ratio, logistic regression, artificial neural networks and their comparison: a case study from Kat landslides (Tokat—Turkey). *Computers and Geosciences* 35, 1125-1138.
- Zare, M., Pourghasemi, H. R., Vafakhah, M., Pradhan, B. 2013. Landslide susceptibility mapping at Vaz Watershed (Iran) using an artificial neural network model: a comparison between multilayer perceptron (MLP) and radial basic function (RBF) algorithms. *Arabian Journal of Geosciences* 6, 2873-2888.
- Zine El Abidine, R., Abdelmansour, N. 2019. Landslide susceptibility mapping using information value and frequency ratio for the Arzew sector (North-Western of Algeria). *Bulletin of the Mineral Research and Exploration* 160, 197-211.